p22 Is a Novel Plasminogen Fragment with Antiangiogenic Activity†

Mijung Kwon,‡ Chang-Soon Yoon,‡ Sandra Fitzpatrick,‡ Geetha Kassam,‡ Kenneth S. Graham,§ Mary K. Young,§ and David M. Waisman*,‡

Cancer Biology Research Group, Departments of Biochemistry & Molecular Biology and Oncology, University of Calgary, Calgary, Alberta, Canada T2N 4N1, and Beckman Research Institute of the City of Hope, Duarte, California 91010

Received June 26, 2001; Revised Manuscript Received August 21, 2001

ABSTRACT: Tumor or tumor-associated cells cleave circulating plasminogen into three or four kringle-containing antiangiogenic fragments, collectively referred to as angiostatin. Angiostatin blocks tumor growth and metastasis by preventing the growth of endothelial cells that are critical for tumor vascularization. Here, we show that cancer and normal cells convert plasminogen into a novel 22 kDa fragment (p22). Production of this plasminogen fragment in a cell-free system has allowed characterization of the structure and activity of the protein. p22 consists of amino acid residues 78−180 of plasminogen and therefore embodies the first plasminogen kringle (residues 84−162) as well as additional N- and C-terminal residues. Circular dichroism and intrinsic fluorescence spectrum analysis have defined structural differences between p22 and recombinant plasminogen kringle 1 (rK1), therefore suggesting a unique conformation for kringle 1 within p22. Proliferation of capillary endothelial cells but not cells of other lineages was selectively inhibited by p22 in vitro. In addition, p22 prevented vascular growth of chick chorioallantoic membranes (CAMs) in vivo. Furthermore, administration of p22 at low dose suppressed the growth of murine Lewis lung carcinoma (LLC) metastatic foci in vivo. This is the first identification of a single kringle-containing antiangiogenic plasminogen fragment produced under physiological conditions.

Plasminogen is converted to the active two-chain form, plasmin, by the cleavage of Arg^{561}−Val^{562} bond by tissue plasminogen activator (t-PA)[1] or urokinase-type plasminogen activator (u-PA). Disulfide bridges form covalent bonds that link the two polypeptide chains of plasmin together. Each polypeptide chain represents a distinct functional domain of plasmin. The larger polypeptide chain or A chain (Lys^{78}−Arg^{561}) contains five kringle domains while the smaller polypeptide chain or B chain (Val^{562}−Asn^{791}) contains the serine proteinase domain. The kringles of the A chain function to mediate protein−protein interactions, such as those between plasminogen and its cell-surface receptors. Recently, it has been shown that plasmin can be further degraded to three or four kringle-containing A chain fragments. Since these plasminogen fragments have antiangiogenic activity, they have been referred to as angiostatin.

Folkman's group recently proposed that a primary tumor, while capable of stimulating angiogenesis in its own vascular bed, could inhibit angiogenesis in the vascular bed of metastatic or other secondary tumors (reviewed in ref *1*). The angiogenesis inhibitors produced by the primary tumor, because of their longer half-life in the circulation, were postulated to reach the vascular bed of the secondary tumor in excess of angiogenic stimulators, thus resulting in the inhibition of the growth of metastatic or secondary tumor. Folkman's group demonstrated that the urine of mice bearing LLC contained an angiogenesis-inhibiting substance that suppressed neovascularization and hence the growth of lung metastases. This urine factor was purified and named angiostatin (*2*, *3*). Mouse angiostatin was shown to be a 38 kDa internal proteolytic fragment of plasminogen consisting of the first three kringle domains of the protein. The purified mouse angiostatin was shown to both suppress the growth of primary LLC in vivo and potently inhibit the proliferation of bovine capillary endothelial (BCE) cells in vitro. Subsequently, Folkman's group prepared a plasminogen fragment from porcine pancreatic elastase digests of human plasminogen that inhibited the proliferation of BCE cells as well as the growth of several human primary carcinomas in mice (*4*). This human angiostatin comprised proteins of 38−45 kDa and consisted of the first three kringles of plasminogen, presumably Tyr^{80}−$Val^{338/354}$ (*5*, *6*). Later, Folkman's group prepared a second plasminogen fragment with angiostatin activity. This second form of human angiostatin was reported to be composed of the first four kringles of plasminogen and comprised the amino acid sequence Lys^{78}−Ala^{440} (*7*). Subsequently, a variety of plasminogen fragments with antiangiogenic activity have been identified. Recently, we

† This work was supported by a grant from the Medical Research Council of Canada.

* To whom correspondence should be addressed. Tel: (403) 220-3022. Fax: (403) 283-4841. E-mail: waisman@ucalgary.ca.

‡ University of Calgary.

§ Beckman Research Institute of the City of Hope.

[1] Abbreviations: p22, plasminogen fragment defined by the amino acid sequence Lys^{78}−Lys^{180}; t-PA, tissue plasminogen activator; u-PA, two-chain urokinase-type plasminogen activator; LLC, Lewis lung carcinoma; BCE cells, bovine capillary endothelial cells; A_{61}, plasminogen fragment defined by the amino acid sequence Lys^{78}−Lys^{468}; rK1, recombinant kringle 1 of plasminogen; HUVECs, human umbilical vein endothelial cells; DMEM, Dulbecco's modified Eagle's medium; CD, circular dichroism; AMCHA, *trans*-4-(aminomethyl)cyclohexanecarboxylic acid; PBS, phosphate-buffered saline (137 mM NaCl, 8 mM Na_2HPO_4, 1.4 mM KH_2PO_4, 2.7 mM KCl, pH 7.4); TPBS, phosphate-buffered saline containing Tween-20 (137 mM NaCl, 8 mM Na_2HPO_4, 1.4 mM KH_2PO_4, 2.7 mM KCl, pH 7.4, and 0.1% Tween-20); CAM, chick chorioallantoic membrane.

10.1021/bi0113420 CCC: $20.00
Published on Web 10/13/2001

have demonstrated that normal and cancer cells produce an antiangiogenic plasminogen fragment that comprises the amino acid sequence $Lys^{78}-Lys^{468}$ (A_{61}) (*8*).

In the present report we demonstrate that plasminogen binds to the surface of BCE cells or human HT1080 fibrosarcoma cells and is subsequently converted to a novel single kringle-containing fragment of M_r 22 000 that we have named p22. N-Terminal sequencing analysis has shown that the N-termini of p22 and plasmin are identical, indicating that p22 is derived from the N-terminal region of plasmin. We have generated p22 in a cell-free system and established that p22 encompasses four regions which include six N-terminal residues, plasminogen kringle 1, three residues of the kringle 1−kringle 2 linker region, and 15 residues of plasminogen kringle 2 (Figure 3). Interestingly, comparison of p22 with purified rK1 has shown that p22 is biochemically distinct from rK1. This suggests that the additional amino acids unique to p22 modulate the structure and activity of the kringle domain of p22. We have also demonstrated that p22 is a potent antiangiogenic protein. The discovery of a single kringle-containing antiangiogenic plasminogen fragment, produced under physiological conditions, should facilitate studies of the mechanism of action of plasminogen-based antiangiogenic proteins.

EXPERIMENTAL PROCEDURES

Materials. Two-chain urokinase-type plasminogen activator (u-PA) was a generous gift from Dr. H. Stack (Abbott Laboratories). [Glu]plasminogen was purified from outdated pooled human plasma by affinity chromatography according to ref *9*. Both isoforms of [Glu]plasminogen were used in the experiments described herein. The recombinant kringle 1 of plasminogen (rK1) was a generous gift from Dr. M. Llinas (Department of Chemistry, Carnegie Mellon University, Pittsburgh, PA) (*10*). Monoclonal anti-human plasminogen kringle 1−3 antibody was purchased from Enzyme Research Laboratories Inc. Anti-mouse horseradish peroxidase-conjugated secondary antibody was purchased from Santa Cruz Biotechnology. Cell lines were obtained from the following sources: HT1080 fibrosarcoma cells, Lewis lung carcinoma cells (LLC), 293 cells, and HeLa cells from American Type Culture Collection; bovine capillary endothelial (BCE) cells from Clonetics. Human umbilical vein endothelial cells (HUVECs) were a generous gift from Dr. Kamela Patel (University of Calgary). Dulbecco's modified Eagle's medium (DMEM) was purchased from GIBCO-BRL and JRH Biosciences. Isoton II solution was obtained from Beckman Coulter. Acetonitrile, ethyl acetate, and heptane were purchased from Burdick and Jackson. Diphenyl chlorophosphate, potassium thiocyanate, pyridine, pentanesulfonic acid, phosphoric acid, and all other organic solvents were purchased from Aldrich. Reagent 4R and the amino acid thiohydantoin standard mixture for the HP G1000A were purchased from Hewlett-Packard.

Cell-Mediated Generation of p22. HT1080 cells were maintained in DMEM (GIBCO-BRL) supplemented with 10% heat-inactivated fetal bovine serum, 2 mM L-glutamine, 10 units/mL penicillin G, and 10 μM streptomycin sulfate. Approximately 1×10^5 cells in 1 mL were added to each well of 24-well tissue culture plates and incubated at 37 °C for 24 h. The cell monolayers were then washed three times with DMEM, and 0.5−8 μM [Glu]plasminogen in DMEM was added to each well. After overnight incubation, the medium was removed, diluted with SDS−PAGE sample buffer with β-mercaptoethanol, and subjected to SDS−PAGE followed by Western blot with monoclonal anti-human plasminogen kringle 1−3 antibody as indicated below.

Purification of Antiangiogenic Plasminogen Fragment (A_{61}). Antiangiogenic plasminogen fragment (A_{61}) was purified as outlined previously (*8*). [Glu]plasminogen (40 μM) was incubated in a buffer containing 50 mM Tris (pH 9.0), 20 mM L-lysine, 100 mM NaCl, 1 mM EDTA, and 0.17 μM two-chain u-PA. The reaction mixture was incubated at 37 °C overnight, diluted 4-fold with 20 mM Hepes (pH 7.4) and 140 mM NaCl, adjusted to 1 mM diisopropyl fluorophosphate (DIFP), and applied to an L-lysine−Sepharose column previously equilibrated with 20 mM Hepes (pH 7.4) and 140 mM NaCl. After a five-column volume wash with the equilibration buffer, the column was subjected to a linear gradient of 0−125 mM 6-aminohexanoic acid (ϵ-ACA), and a single protein peak was eluted, pooled, and concentrated by ultrafiltration. The protein peak was applied to a Sephacryl S-100 column previously equilibrated with 20 mM Hepes (pH 7.4) and 140 mM NaCl, and the single protein peak was pooled. Typically 51 mg of A_{61} was recovered from 100 mg of [Glu]plasminogen.

p22 Generation. A_{61} (7 μM) was incubated with 0.1 μM plasmin in a buffer containing 20 mM Hepes (pH 7.4), 140 mM NaCl, and 100 μM dithiothreitol at 37 °C for 2 h. The reaction was stopped by addition of 1 mM Pefabloc, and the reaction mixture was applied to an L-lysine−Sepharose column previously equilibrated with 20 mM Hepes (pH 7.4) and 140 mM NaCl. The flow-through fraction was loaded onto an octyl-Sepharose resin previously equilibrated with 20 mM Hepes (pH 7.4) and 4 M NaCl. The purified p22 protein, present in the flow-through fraction, was dialyzed against 20 mM Hepes (pH 7.4) and 20 mM NaCl. The dialyzed p22 protein was aliquoted and frozen at −80 °C until use.

Immediately before use in the endothelial cell proliferation assay, aliquots of p22 were applied to a Detoxi-Gel column (Pierce), and endotoxin was removed according to the manufacturer's instructions. Endotoxin contamination of the purified p22 was analyzed by Pyrotell *Limulus* amebocyte lysate assay (Associates of Cape Cod Inc., Falmouth, MA) and was found to be less than 40 pg of endotoxin/mL (0.4 EU/mL).

Electrophoresis and Western Blot. Samples were diluted with SDS−PAGE sample buffer and subjected to SDS−PAGE (*11*). Proteins were transferred to a 0.45 μm pore size nitrocellulose membrane at 4 °C for 1 h. The membrane was blocked in TPBS (phosphate-buffered saline containing 0.1% Tween-20) with 5% skim milk at room temperature for 1 h and incubated at 4 °C overnight in TPBS with 5% skim milk and a 1:2500 dilution of 1 mg/mL monoclonal anti-human plasminogen kringle 1−3 antibody. The blot was extensively washed with TPBS at room temperature and then incubated at room temperature for 1 h with a 1:2500 dilution of horseradish peroxidase-conjugated goat anti-mouse secondary antibody in TPBS with 5% skim milk. The membrane was extensively washed with TPBS, developed with the Supersignal reagent (Pierce), and visualized by chemiluminescence.

Amino- and Carboxyl-Terminal Sequencing of p22. N-Terminal sequence analysis was performed by the University of Calgary Sequence Analysis Facility and the Alberta Peptide Institute (University of Alberta). C-Terminal sequence analysis was performed by the Beckman Research Institute of the City of Hope (Duarte, CA). p22 was sequenced using a Hewlett-Packard HP G1000A C-terminal protein sequencer and an Applied Biosystems 477C Procise C C-terminal sequencer.

Measurement of Molecular Mass by Mass Spectrometry. Mass spectrometry was performed by the Beckman Research Institute of the City of Hope (Duarte, CA). Matrix-assisted laser desorption ionization (MALDI) mass spectra were obtained using a Voyager DE-STR (PE Biosystems) MALDI time-of-flight mass spectrometer (MS).

Intrinsic Fluorescence Measurements. Excitation and emission spectra were collected with a Perkin-Elmer LS 50B fluorescence spectrometer equipped with a constant-temperature cell holder. The excitation and emission slit widths were set to 5 and 10 nm, respectively. The spectra were collected at 20 °C with p22 (25 μM) or rK1 (10 μM) in a buffer consisting of 20 mM HEPES (pH 7.4) and 140 mM NaCl in the presence or absence of ligand. The data were corrected for the slight dilution consequent to ligand additions.

Circular Dichroism. Circular dichroism (CD) measurements were performed with a Jasco J-810 spectropolarimeter. The spectropolarimeter was calibrated with an aqueous solution of recrystallized ammonium camphorsulfonate-10-*d*. p22 (41 μM) or rK1 (25 μM) in a buffer containing 10 mM Tris (pH 7.5) and 150 mM NaCl was scanned in a quartz cuvette (0.5 mm path length) from 178 to 260 nm at a rate of 20 nm/min, using a bandwidth of 1 nm and a response time of 4 s. CD spectra of proteins were obtained by averaging five wavelength scans and were corrected by subtracting buffer scans. Results are expressed as $\Delta\epsilon$ ($M^{-1}\cdot cm^{-1}$). The predicted secondary structure content of p22 was assessed with the program CDsstr version 1.8 (*12*).

Endothelial Cell Proliferation Assay. BCE cells were maintained in DMEM (JRH Biosciences) supplemented with 10% heat-inactivated calf serum, 2 mM L-glutamine, 10 units/mL penicillin G, 10 μM streptomycin sulfate, and 3 ng/mL basic fibroblast growth factor (Calbiochem). BCE cells (passage 3−5) were plated into 24-well tissue culture plates (3000 cells/well) and incubated at 37 °C for 24 h. The medium was replaced with fresh DMEM containing 5% calf serum in the presence or absence of p22 or rK1. After a 30 min incubation, basic fibroblast growth factor was added to a final concentration of 1 ng/mL, and cells were further incubated for 72 h. The cells were trypsinized and resuspended in Isoton II solution, and the cell number was determined with a Coulter counter.

Chick Chorioallantoic Membrane (CAM) Assay. Three-day-old fertilized white Leghorn eggs (Lillydale, Calgary, AB) were cracked, and chick embryos with intact yolks were placed in 100 × 20 mm culture dishes. After 3 days of incubation in 5% CO_2 at 37 °C, disks of methylcellulose containing phosphate-buffered saline (PBS: 137 mM NaCl, 8 mM Na_2HPO_4, 1.4 mM KH_2PO_4, and 2.7 mM KCl, pH 7.4) or 5 μg of p22 (50 μL of 8.3 μM) were implanted on the CAM of embryos. After 48 h of incubation, embryos and CAMs were analyzed for the formation of avascular zones under the stereo microscope, and pictures were taken at 40× magnification.

Murine Tumor Model. LLC cells were harvested at log phase and resuspended in PBS. Approximately 10^6 cells were injected subcutaneously in the middle dorsum of 6−8-week-old C57BL/6 male mice. When tumors reached 1500 mm^3 in size (approximately 14 days after implantation), the mice were randomly divided into two groups. The first group underwent surgical resection of the tumor, and the second group was subjected to a sham surgical procedure in which tumors were manipulated but left intact. Animals from the tumor-resected group were randomly placed into test and control groups. The test group of mice received daily intraperitoneal injections of p22 in PBS (dose = 2.5 mg/kg per day, 500 μL of 8.3 μM) while the control group received PBS. After 14 days all mice were sacrificed, the lungs were weighed, and the number of lung metastatic foci was counted.

RESULTS

HT1080 Cells Produce a Novel Plasminogen Fragment. The cell-mediated formation of the broad-spectrum proteinase, plasmin, requires the binding of plasminogen and its activators, t-PA or u-PA, to the extracellular surface (*13*−*15*). The localization of plasminogen and its activators at the cell surface results in the conversion of plasminogen to plasmin. Recently, it has been demonstrated that the binding of plasminogen or plasmin to the cell surface also results in the formation of plasmin(ogen) fragments of M_r ~66 000, ~60 000, and ~57 000. These plasmin(ogen) fragments, typically consisting of the first four kringles of plasminogen, have antiangiogenic activity and have therefore been referred to as angiostatin (*16*−*18*).

Incubation of human [Glu]plasminogen with HT1080 human fibrosarcoma cells resulted in the generation of antiangiogenic plasminogen fragment (A_{61}) and a novel plasminogen fragment of approximate M_r 22 000 in reduced SDS−PAGE (Figure 1A). Furthermore, upon varying the concentration of plasminogen, the amount of cell-generated p22 increased in a dose-dependent manner. Importantly, the generation of p22 was observed at the concentration of plasminogen as low as 1 μM, well within the physiological concentration of circulating plasminogen. The p22 protein was detected due to its reactivity with a monoclonal antibody to the first three kringles of plasmin(ogen). In addition, similar results were obtained when [Lys]plasminogen was used instead of [Glu]plasminogen (Figure 1B). As shown in Figure 1C, other cells such as bovine capillary endothelial (BCE) cells and HeLa cells also converted plasminogen to p22. However, human umbilical vein endothelial cells (HUVECs) did not generate detectable p22 under the same experimental condition. Furthermore, based on its mobility in reduced SDS−PAGE it was evident that p22 was slightly larger than rK1, yet smaller than the M_r of 38 000 or 25 000 determined for recombinant kringle 1−3 or recombinant kringle 2−3, respectively. It was therefore likely that p22 was a single kringle-containing plasminogen fragment.

To identify the region of plasmin(ogen) that was cleaved to produce p22, we subjected the HT1080 cell-generated p22 to N-terminal sequence analysis. The N-terminus of p22 corresponded to Lys^{78} of plasminogen. Furthermore, since p22 is larger than the rK1 of plasmin(ogen) (Figure 1C) and

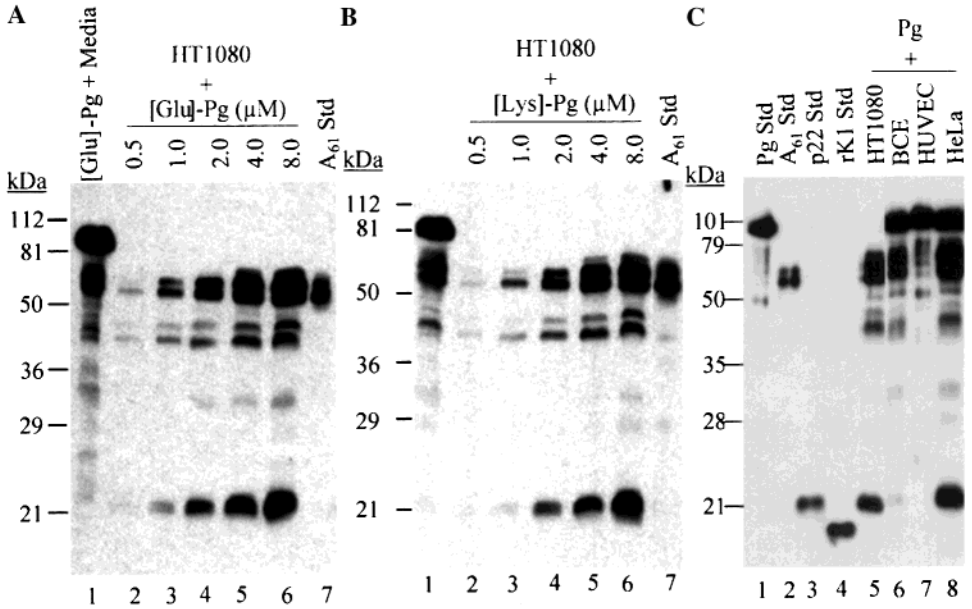

FIGURE 1: Identification of a novel plasminogen fragment produced by HT1080 cells. (A) HT1080 cells were incubated with DMEM containing the indicated concentrations of [Glu]plasminogen (Pg). After an overnight incubation, the medium was analyzed by 15% reduced SDS−PAGE followed by Western blot with monoclonal anti-human plasminogen kringle 1−3 antibody. [Glu]plasminogen (8 μM) after overnight incubation in the absence of cells (lane 1), and A_{61} standard (lane 7). The HT1080 cells were incubated with the following concentrations of [Glu]plasminogen; 0.5 μM (lane 2); 1 μM (lane 3); 2 μM (lane 4); 4 μM (lane 5); 8 μM (lane 6). (B) HT1080 cells were incubated with DMEM containing the indicated concentrations of [Lys]plasminogen (K-Pg) as indicated in (A). (C) HT1080 (lane 5), BCE (lane 6), or HUVECs (lane 7) were incubated with DMEM containing 8 μM [Glu]plasminogen, and after an overnight incubation the medium was subjected to 12.5% reduced SDS−PAGE followed by Western blot with monoclonal anti-human plasminogen kringle 1−3 antibody. [Lys]plasminogen was used in the case of HeLa cells (lane 8). The following standards are also shown: plasminogen (lane 1); A_{61} (lane 2); p22 (lane 3); rK1 (lane 4).

p22 is detected with anti-plasminogen kringle 1−3 antibody, we have concluded that p22 consists of the kringle 1 of plasmin(ogen) and several additional N- and C-terminal residues. Thus, p22 is a novel plasminogen fragment.

Generation of p22 in Vitro. To obtain sufficient quantities of p22 for biochemical analysis, we attempted to produce p22 in a cell-free system. Previous work from our laboratory had established that plasmin autodigestion resulted in the generation of a novel antiangiogenic fragment of M_r 61 000, called A_{61}, that consisted of the amino acid sequence Lys^{78}−Lys^{468} and therefore was composed of kringle domains 1−4 and part of kringle 5 (*8*). As shown in Figure 2, we have observed that when A_{61} was incubated with plasmin and the reducing reagent dithiothreitol, p22 and other plasminogen fragments were generated from the subsequent degradation of A_{61}. Subsequent purification of the reaction mixture resulted in the isolation of milligram quantities of p22. The p22 produced by cell-free system was indistinguishable on SDS−PAGE from the p22 produced by incubation of plasminogen with HT1080 cells (Figure 1C).

Characterization of p22. N-Terminal sequence analysis of the p22 generated in our cell-free system established that the N-terminus corresponded to the region of human plasminogen Lys^{78}−Ser^{82}. The N-terminus of the p22 generated in the cell-free system was therefore identical to that of the HT1080 cell-generated p22. C-Terminal sequence analysis of the p22 generated in the cell-free system identified Lys^{177}−Lys^{180} of plasminogen as the last four residues of the C-terminus of p22 (Table 1). The N- and C-terminal sequencing therefore established that the p22 was formed by the cleavage of plasminogen at two sites, Lys^{77}−Lys^{78} and Lys^{180}−Thr^{181}. Therefore, p22 is a novel plasminogen

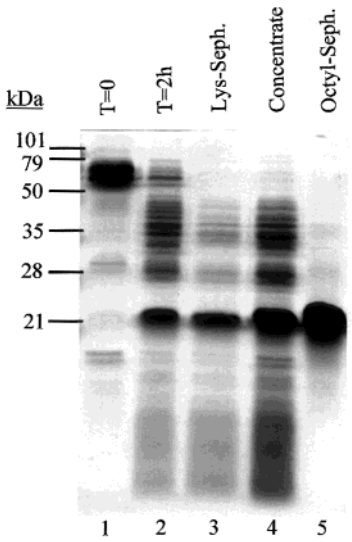

FIGURE 2: Generation of p22 in a cell-free system. Antiangiogenic plasminogen fragment (A_{61}) (lane 1) was purified as indicated in the Experimental Procedures. A_{61} (7 μM) was incubated with plasmin (0.1 μM) and dithiothreitol (100 μM) at 37 °C for 2 h (lane 2). p22 was purified by L-lysine−Sepharose column chromatography (lane 3), concentrated (lane 4), and further purified by octyl-Sepharose column chromatography (lane 5). Samples were subjected to SDS−PAGE, and protein bands were visualized after staining with Coomassie blue.

fragment that has the primary amino acid sequence of Lys^{78}−Lys^{180}. Thus, p22 is composed of six N-terminal residues, plasminogen kringle 1, three residues of the kringle 1−kringle 2 linker region, and 15 residues of kringle 2 (Figure 3). The average M_r measured from this amino acid sequence was 11 825, which compared favorably with the M_r 11 821 derived from mass spectrometry of p22. The similarity of

Table 1: Amino- and Carboxyl-Terminal Sequence of Human p22[a]

plasminogen p22 C-sequence	G^{176}	K^{177} K	I^{178} I	S^{179} S	K^{180} K	T^{181}
plasminogen p22 N-sequence	K^{78} K	V^{79} V	Y^{80} Y	L^{81} L	S^{82} S	

[a] Human p22 was generated from the human antiangiogenic plasminogen fragment (A_{61}), plasmin, and dithiothreitol in the cell-free system as described in the Experimental Procedures.

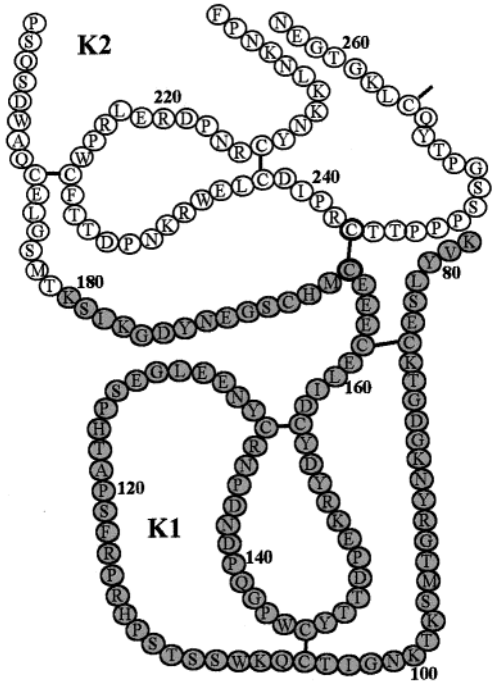

FIGURE 3: Diagrammatic illustration of the structure of p22. The amino acids are indicated with the single letter code. The shaded region represents the structure of p22.

the molecular weight of p22 calculated from the amino acid sequence with that of the molecular weight derived from mass spectrometry rules out the possibility of glycosylation or other posttranslational modifications of p22. By comparison, the M_r of rK1 was 9815 by mass spectrometry and 9926 as calculated from the amino acid composition.

The intrinsic fluorescence excitation and emission maxima of p22 were 283 and 332 nm, respectively (Figure 4A). By contrast, the intrinsic fluorescence excitation and emission maxima of rK1 were 283 and 339 nm, respectively. The binding of the lysine analogue, *trans*-4-(aminomethyl)-cyclohexanecarboxylic acid (AMCHA), to p22 caused a significant increase (22%) in the intrinsic fluorescence emission spectra. Furthermore, although rK1 also showed a large increase in intrinsic fluorescence emission spectra of 20% upon binding to AMCHA, the emission maximum was blue shifted from 339 to 331 nm. These results establish that the kringle domain of p22 is conformationally distinct from rK1. Therefore, amino acids of the N- or C-terminal domains of p22 probably interact with and modulate the structure of the kringle domain of p22.

We also examined the CD spectra of p22 and rK1. The CD spectrum of rK1 exhibited a positive band at 227.5 nm and a strong negative band at 197.4 nm (Figure 4B). The overall shape of the CD spectrum of p22 was distinct from that of rK1. The spectrum of p22 showed a positive band at 227.5 nm and strong negative band at 202.7 nm, which was

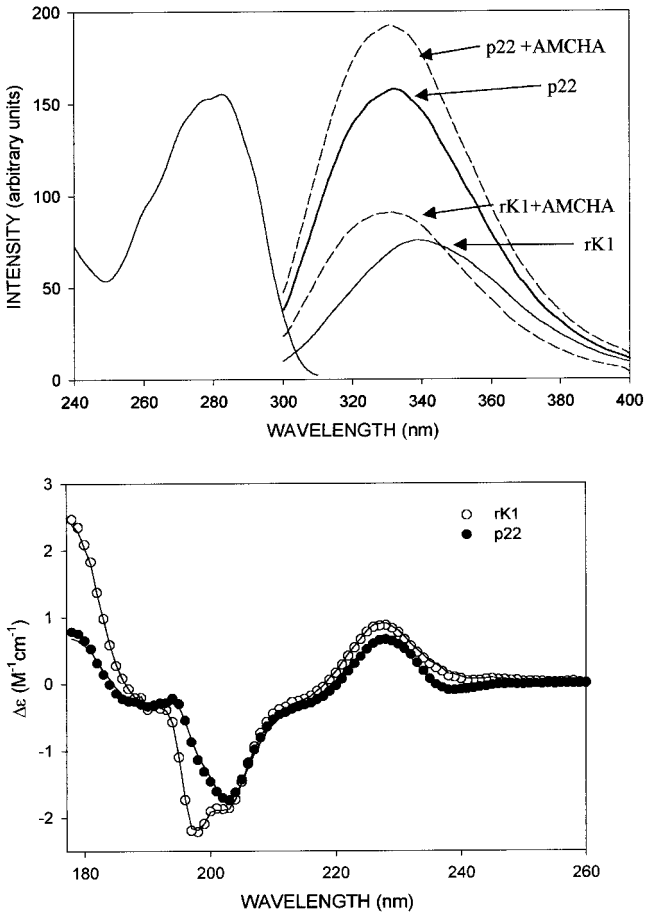

FIGURE 4: Spectroscopic analysis of p22 and rK1. (A) Intrinsic fluorescence spectra of p22 and rK1. The excitation (ex) and emission spectrum (em) of ligand-free (solid line) and AMCHA (1 mM) saturated p22 and rK1 (dotted line) are presented. The spectrum was measured at 20 °C in 20 mM HEPES (pH 7.4) and 140 mM NaCl. The concentrations of p22 and rK1 were 25 and 10 μM, respectively. (B) CD spectra of p22 and rK1. Wavelength scans were conducted at 20 °C in 10 mM Tris (pH 7.5) and 150 mM NaCl. The concentrations of p22 and rK1 were 41 and 25 μM, respectively. The line through the points represents the best fit for the data reconstructed from the average of the calculated combinations of secondary structure content.

Table 2: Comparison of the Secondary Structure of p22 and rK1[a]

structure	p22	rK1
α helix	0	3
3_{10} helix	3	3
β sheet	21	25
β turns	15	7
3_1 helix	17	19
unordered	43	42

[a] CD scans were conduced at 20 °C in buffer containing 10 mM Tris (pH 7.5) and 150 mM NaCl. Predicted secondary structure assignments were obtained from analysis of CD spectra using the computer program CDsstr version 1.

characteristic of a protein devoid of α-helical structure. The negative ellipticity near 200 nm was consistent with the presence of poly(pro)II helices (3_1 helices) within the secondary structure of p22. Indeed, estimation of the secondary structure content of p22 by the variable selection method (*12*) (Table 2) suggested that p22 was composed of approximately 17% 3_1 helix.

Biological Activity of p22. A number of different plasminogen fragments including the kringle1−3 and kringle 1−4

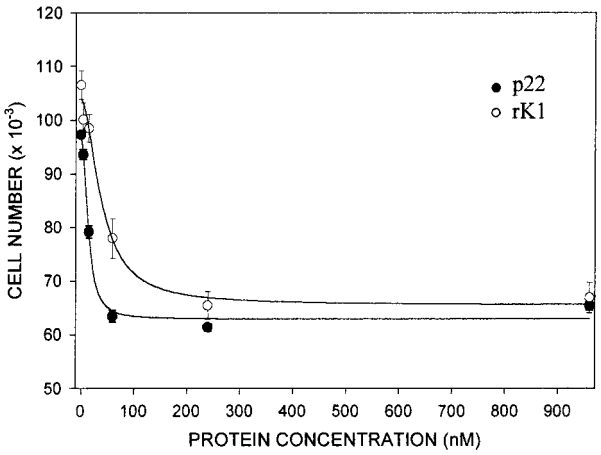

FIGURE 5: Inhibition of bovine capillary endothelial cell proliferation by p22 and rK1. BCE cells were incubated with various concentrations of p22 or rK1 in the presence of 1 ng/mL basic fibroblast growth factor. After 72 h incubation, the cells were trypsinized, resuspended in Isoton II solution, and counted with a Coulter counter.

regions of plasminogen have been demonstrated to possess antiangiogenic activity. We therefore examined p22 for possible antiangiogenic activity. p22 inhibited BCE cell growth in a dose-dependent manner (Figure 5). The concentration of p22 required for 50% inhibition (IC_{50}) was 14.3 ± 2.3 nM (mean ± SD, $n = 3$), and maximum inhibition was observed at a concentration of about 50 nM. The IC_{50} of p22 was lower than the IC_{50} of 35 nM reported for A_{61} (*8*) and 39.5 ± 9.7 nM (mean ± SD, $n = 3$) determined for rK1. We also found that concentrations of p22 as high as 2 μM did not inhibit the proliferation of several nonendothelial cell lines such as HT1080 fibrosarcoma cells, HeLa cells, and 293 cells (data not shown).

To determine whether p22 possesses antiangiogenic activity in vivo, we examined the effect of p22 on de novo growth of blood vessels on chick chorioallantoic membranes (CAMs). Compared with the PBS control, 5 μg of p22 prevented vascular growth under these conditions (Figure 6). These results further suggest that p22 is an antiangiogenic protein.

We also examined the antimetastatic activity of p22 in the murine tumor model. C57BL/6 mice were inoculated with LLC cells, and after 14 days the primary tumor was resected. One group of mice received daily intraperitoneal injections of p22 in PBS (dose = 2.5 mg/kg per day), while the control group received PBS. We determined the number of metastatic foci that were observable in the lung tissue after resection of the primary tumor. The lungs of mice treated with PBS after tumor resection had 38 ± 4 (mean ± SD, $n = 18$) metastatic foci while mice treated with p22 had only 3 ± 2 (mean ± SD, $n = 18$) metastatic foci (Figure 7A,C). The lung weight of mice with the primary tumor resected and treated with PBS increased over time and 14 days after primary tumor resection had reached 646.5 ± 123 mg (mean ± SD, $n = 18$) (Figure 7B,C). In contrast to the lung weight of mice treated with PBS, the average lung weight of the mice that had received daily doses of p22 only increased to 191.8 ± 31 mg (mean ± SD, $n = 18$). By comparison, the average weights of the lungs from normal mice or 14-day primary tumor-bearing mice were 191 ± 25 mg (mean ± SD, $n = 5$) and 199 ± 20 mg (mean ± SD, $n = 10$), respectively. These results suggest that p22 also has a potent antimetastatic activity possibly due to its antiangiogenic activity.

DISCUSSION

An emerging concept in biology is that certain inactive precursor proteins are cleaved in vivo to produce biologically active fragments. For example, the serine protease kallikrein cleaves kininogen, resulting in the release of bradykinin, a potent vasodilator (*19*). Similarly, the proteolysis of collagen XVIII results in the generation of endostatin, a potent antiangiogenic protein (*20*). This concept of bioregulatory proteolysis is dramatically illustrated for plasminogen where the proteolytic cleavage of the molecule produces the broad spectrum protease plasmin. The further cleavage of plasmin produces antiangiogenic plasminogen fragments typically consisting of the first three or four kringles. Although many different plasminogen fragments have been produced in vitro by the proteolytic digestion of plasmin(ogen) or by recombinant technology, it has been unclear which antiangiogenic plasminogen fragments are produced under physiological conditions.

In a previous study we demonstrated that the incubation of cells with plasminogen results in the generation of a plasminogen fragment comprising the first four kringles and part of the fifth kringle, Lys^{78}–Lys^{468} (*8*). Furthermore, we demonstrated that this plasminogen fragment, called A_{61}, was

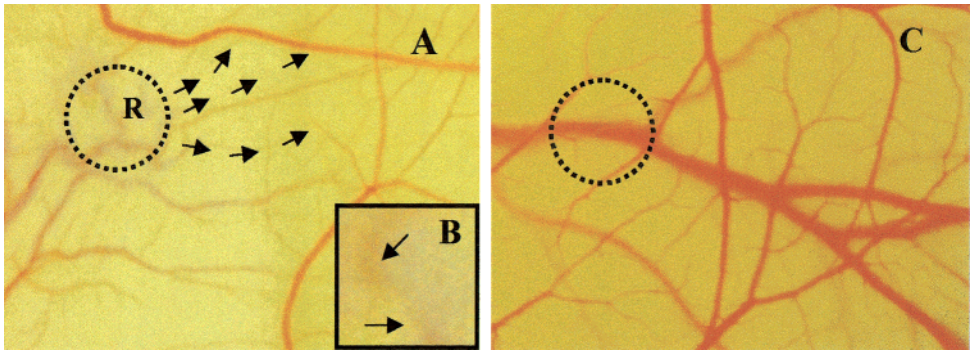

FIGURE 6: Inhibition of neovascularization on the chick chorioallantoic membrane (CAM) by p22. Methylcellulose disks containing PBS or 5 μg of p22 were implanted on the CAM of 6-day-old chick embryos. After 48 h, the formation of avascular zones was analyzed. The pictures are representative of 10 experiments. The dotted circles in panels A and C indicate the position of the methylcellulose disks. (A) A CAM treated with a methylcellulose disk containing p22. The area of the avascular zone is marked by arrows. (B) The high-magnification insert of the area marked by R in panel A shows the regressed vessels (arrows) in the adjacent area of the avascular zone. (C) A control CAM with a methylcellulose disk containing PBS.

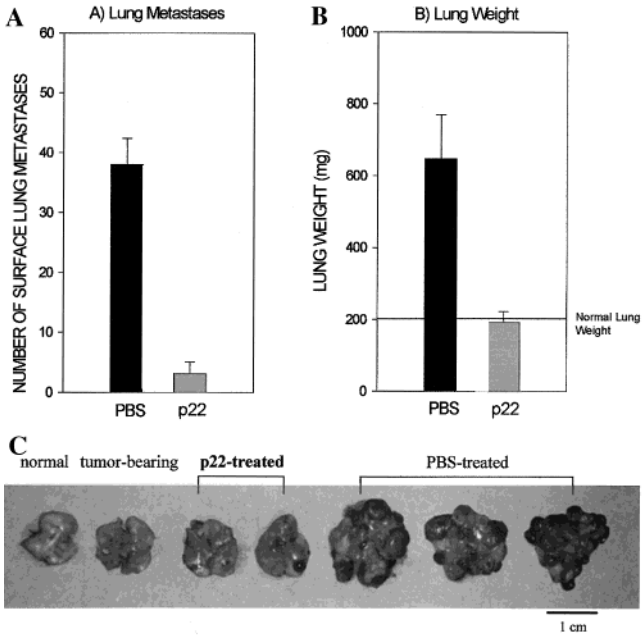

FIGURE 7: Inhibition of metastatic tumor growth in mice lungs. Mice were injected intraperitoneally with PBS or p22 (in PBS) (2.5 mg/kg per day) immediately after removal of the primary tumor. p22 treatment inhibited the growth of metastatic foci (A) and blocked an increase in lung weight (B) after removal of the primary tumor. (C) Visual comparison of PBS- or p22-treated mice lungs at 14 days after resection of the primary tumor. Lungs from normal and primary tumor-bearing mice are also shown.

present in the serum of normal and tumor-bearing patients. We concluded from our studies that A_{61} was produced from plasmin autoproteolysis. In the current study we have refined our analysis and shown that cells can also convert plasminogen into a novel single kringle-containing plasminogen fragment that we have named p22 (Figure 3).

The kringles are small protein domains that consist of about 80 amino acids and have a characteristic three disulfide-bonded structure. These domains appear to be independently folded units that have been defined structurally to have a cysteine residue at their N- and C-terminus. The kringle domains appear singly in u-PA (*21*) and factor XII (*22*), twice in t-PA and prothrombin (*23*), four times in hepatocyte growth factor (*24*), five times in plasminogen, and about 40 times in apolipoprotein(a) (*25*−*27*). One of the key structures within a kringle is its lysine-binding site. In general, the lysine-binding site of a kringle interacts with the C-terminal lysine of the target protein. For example, the kringle domains of plasminogen are presumed to interact with fibrin by binding to an exposed lysine side chain. Furthermore, the kringle domains of plasminogen bind to the cell surface via their binding to the C-terminal lysines of receptor proteins such as annexin II tetramer or to α_2-antiplasmin, the major plasma inhibitor of plasmin (*28*−*30*). There is also evidence that the kringles are capable of mediating intramolecular interactions by interacting with intrachain lysine residues (*31*−*34*).

The individual plasminogen kringles have been produced by recombinant technology and extensively studied. Although these structures have 48−50% identity, they are not functionally equivalent. For example, the binding affinities of the kringles for *N*-acetyl-L-lysine, which models the structure of a C-terminal lysine, are in order of decreasing affinity of kringle 1 > kringle 4 > kringle 2. The kringle 5 only weakly binds this lysine analogue while kringle 3 is incapable of binding it (*35*). Interestingly, kringle 1, kringle 2, kringle 4, and kringle 5 have similar affinity for lysine analogues that mimic an intrachain lysine (*35*). The plasminogen kringles may have distinct binding partners in vivo. Kringle 2 exclusively binds to intrachain lysines of the group A streptococcal surface protein, PAM (*35*). Likewise, kringle 4 exclusively interacts with the C-terminal lysine residue of α_2-antiplasmin (*30*). On the basis of this information it is reasonable to suspect that p22 may have a unique binding site on the endothelial cell surface compared to other multiple kringle-containing antiangiogenic plasminogen fragments. It is also not clear at this time if the mechanism of action of p22 is similar to other antiangiogenic plasminogen fragments.

To date, p22 is the smallest plasminogen fragment shown to be generated under physiological conditions. Since p22 contains only a single kringle domain, future structure−function analysis of the antiproliferative activity of this protein will be simpler than similar studies of the multiple kringle-containing plasminogen fragments such as A_{61}. Since the individual kringles of plasminogen have been expressed as recombinant proteins, it is possible to compare their biological activities with that of p22. The individual plasminogen kringle domains have distinct antiproliferative activities as measured by the endothelial cell proliferation assay. Kringle 5, kringle 1, and kringle 3 exhibit potent inhibitory activity, kringle 2 displays weaker activity, while kringle 4 is not effective (*7*, *36*). These kringles also have discrete inhibitory functions on endothelial cell migration with kringle 5 and kringle 4 showing potent activity, kringle 2 and kringle 3 showing lesser inhibitory activity, and kringle 1 showing negligible activity (*37*, *38*). Interestingly, while the structural integrity of the kringles appears to be necessary for their inhibitory activities, the lysine binding site of the kringle does not appear to be involved with this function (*7*, *37*).

In the current study we showed that both rK1 and p22 block the proliferation of capillary endothelial cells. In addition, we showed that p22 possesses antimetastatic activity in vivo. It was interesting that the conformations of p22 and rK1 were distinct (Figure 4). Of particular interest was our observation that binding of the lysine analogue, AMCHA, to K1 blue shifted the fluorescence emission spectra maximum from 339 to 331 nm. This suggests that one or more Trp have moved into a more hydrophobic environment upon AMCHA binding. In contrast, binding of AMCHA to p22 did not cause a shift in the fluorescence emission spectra maximum from its ligand-free value of 332 nm. The simplest explanation for the differences in the fluorescence spectra is that the lysine-binding kringle domain of p22 interacts with the N-terminal lysine of the N-terminal extension region of p22, and this interaction results in a movement of one or more Trp to a more hydrophobic environment, resulting in a blue shift in the p22 fluorescence emission spectra. The interaction of AMCHA with p22 would then be expected to displace the N-terminal extension and maintain the Trp(s) in a hydrophobic environment, thus maintaining the blue shift in the p22 fluorescence emission spectra. Alternatively, since the extended C-terminal regions of p22 contain an intrachain lysine and C-terminal lysine, it is possible that these residues may interact with the p22 kringle. Furthermore, the major

difference between the CD spectra of p22 and K1 is the increased content of β turns in p22. It is reasonable to speculate that the interactions of the extended N- or C-terminal regions of p22 with the p22 kringle site may have caused the formation of new β turns in the protein. Alternatively, it is also possible that either of the extended regions of p22 may have assumed a conformation rich in β turns. It is reasonable to assume that the new conformation resulting from the postulated interactions between the N- or C-terminal extensions with the kringle domain of p22 may contribute to the increased antiproliferative activity of p22 compared to rK1. Alternatively, it is also possible that the residues of p22 that form the extended N- or C-terminal region do not interact with the kringle domain and are directly responsible for the unique conformation of p22.

The mechanism of cell-dependent production of p22 is unclear. An analysis of the plasminogen fragments produced by incubation of HT1080 cells with plasminogen has indicated that A_{61} is generated before the formation of p22 (data not shown). This suggests that p22 may be produced by the cleavage of A_{61} on the cell surface. Since p22 is produced in vitro by the cleavage of A_{61} by plasmin, it is reasonable to propose that cell-surface plasmin mediates the cleavage of A_{61} to p22. We cannot, however, rule out the possibility that plasminogen is directly converted to p22 by plasmin or other proteinases.

ACKNOWLEDGMENT

We thank Drs. M. Llinas and J. Schaller for providing recombinant kringle 1 of plasminogen.

REFERENCES

1. O'Reilly, M. S. (1997) *EXS 79*, 273−294.
2. O'Reilly, M. S., Holmgren, L., Shing, Y., Chen, C., Rosenthal, R. A., Cao, Y., Moses, M., Lane, W. S., Sage, E. H., and Folkman, J. (1994) *Cold Spring Harbor Symp. Quant. Biol. 59*, 471−482.
3. O'Reilly, M. S., Holmgren, L., Shing, Y., Chen, C., Rosenthal, R. A., Moses, M., Lane, W. S., Cao, Y., Sage, E. H., and Folkman, J. (1994) *Cell 79*, 315−328.
4. O'Reilly, M. S., Holmgren, L., Chen, C., and Folkman, J. (1996) *Nature Med. 2*, 689−692.
5. Sottrup-Jensen, L., Claeys, H., Zajdel, M., Petersen, T. E., and Magnusson, S. (1978) in *Progress in Chemical Fibrinolysis and Thrombosis* (Davidson, J. F., Somana, M., and Desnoyers, P., Eds.) pp 191−209, Raven Press, New York.
6. Takada, A., Sugawara, Y., and Takada, Y. (1988) *Thromb. Res. 50*, 285−294.
7. Cao, Y., Ji, R. W., Davidson, D., Schaller, J., Marti, D., Sohndel, S., McCance, S. G., O'Reilly, M. S., Llinas, M., and Folkman, J. (1996) *J. Biol. Chem. 271*, 29461−29467.
8. Kassam, G., Kwon, M., Yoon, C.-S., Graham, K. S., Young, M. K., Gluck, S., and Waisman, D. M. (2001) *J. Biol. Chem. 276*, 8924−8933.
9. Castellino, F. J., and Powell, J. R. (1981) *Methods Enzymol. 80* (Part C), 365−378.
10. Rejante, M. R., and Llinas, M. (1994) *Eur. J. Biochem. 221*, 939−949.
11. Laemmli, U. K. (1970) *Nature 227*, 680−685.
12. Johnson, W. C. (1999) *Proteins 35*, 307−312.
13. Pollanen, J., Stephens, R. W., and Vaheri, A. (1991) *Adv. Cancer Res. 57*, 273−328.
14. Felez, J., Miles, L. A., Fabregas, P., Jardi, M., Plow, E. F., and Lijnen, R. H. (1996) *Thromb. Haemostasis 76*, 577−584.
15. Stephens, R. W., Pollanen, J., Tapiovaara, H., Leung, K. C., Sim, P. S., Salonen, E. M., Ronne, E., Behrendt, N., Dano, K., and Vaheri, A. (1989) *J. Cell Biol. 108*, 1987−1995.
16. Stathakis, P., Fitzgerald, M., Matthias, L. J., Chesterman, C. N., and Hogg, P. J. (1997) *J. Biol. Chem. 272*, 20641−20645.
17. Gately, S., Twardowski, P., Stack, M. S., Patrick, M., Boggio, L., Cundiff, D. L., Schnaper, H. W., Madison, L., Volpert, O., Bouck, N., Enghild, J., Kwaan, H. C., and Soff, G. A. (1996) *Cancer Res. 56*, 4887−4890.
18. Falcone, D. J., Khan, K. F., Layne, T., and Fernandes, L. (1998) *J. Biol. Chem. 273*, 31480−31485.
19. Schmaier, A. H. (2000) *Curr. Opin. Hematol. 7*, 261−265.
20. O'Reilly, M. S., Boehm, T., Shing, Y., Fukai, N., Vasios, G., Lane, W. S., Flynn, E., Birkhead, J. R., Olsen, B. R., and Folkman, J. (1997) *Cell 88*, 277−285.
21. Gunzler, W. A., Steffens, G. J., Otting, F., Kim, S. M., Frankus, E., and Flohe, L. (1982) *Hoppe Seyler's Z. Physiol. Chem. 363*, 1155−1165.
22. McMullen, B. A., and Fujikawa, K. (1985) *J. Biol. Chem. 260*, 5328−5341.
23. Pennica, D., Holmes, W. E., Kohr, W. J., Harkins, R. N., Vehar, G. A., Ward, C. A., Bennett, W. F., Yelverton, E., Seeburg, P. H., Heyneker, H. L., Goeddel, D. V., and Collen, D. (1983) *Nature 301*, 214−221.
24. Tashiro, K., Hagiya, M., Nishizawa, T., Seki, T., Shimonishi, M., Shimizu, S., and Nakamura, T. (1990) *Proc. Natl. Acad. Sci. U.S.A. 87*, 3200−3204.
25. McLean, J. W., Tomlinson, J. E., Kuang, W. J., Eaton, D. L., Chen, E. Y., Fless, G. M., Scanu, A. M., and Lawn, R. M. (1987) *Nature 330*, 132−137.
26. Castellino, F. J., and McCance, S. G. (1997) *Ciba Found. Symp. 212*, 46−60.
27. Castellino, F. J., and Beals, J. M. (1987) *J. Mol. Evol. 26*, 358−369.
28. Kassam, G., Le, B. H., Choi, K. S., Kang, H. M., Fitzpatrick, S. L., Louie, P., and Waisman, D. M. (1998) *Biochemistry 37*, 16958−16966.
29. Longstaff, C., and Gaffney, P. J. (1991) *Biochemistry 30*, 979−986.
30. Christensen, U., Bangert, K., and Thorsen, S. (1996) *FEBS Lett. 387*, 58−62.
31. Ryan, T. J., and Keegan, M. C. (1985) *Biochim. Biophys. Acta 830*, 187−194.
32. Menhart, N., Hoover, G. J., McCance, S. G., and Castellino, F. J. (1995) *Biochemistry 34*, 1482−1488.
33. McCance, S. G., and Castellino, F. J. (1995) *Biochemistry 34*, 9581−9586.
34. Takada, Y., Urano, T., and Takada, A. (1993) *Thromb. Res. 70*, 151−159.
35. Marti, D. N., Hu, C. K., An, S. S. A., Von Haller, P., Schaller, J., and Llinás, M. (1997) *Biochemistry 36*, 11591−11604.
36. Cao, Y., Chen, A., An, S. A., Ji, R. W., Davidson, D., and Llinas, M. (1997) *J. Biol. Chem. 272*, 22924−22928.
37. Ji, W. R., Barrientos, L. G., Llinas, M., Gray, H., Villarreal, X., DeFord, M. E., Castellino, F. J., Kramer, R. A., and Trail, P. A. (1998) *Biochem. Biophys. Res. Commun. 247*, 414−419.
38. Ji, W. R., Castellino, F. J., Chang, Y., DeFord, M. E., Gray, H., Villarreal, X., Kondri, M. E., Marti, D. N., Llinas, M., Schaller, J., Kramer, R. A., and Trail, P. A. (1998) *FASEB J. 12*, 1731−1738.

BI0113420